MULTI-CELL TEMPERATURE MAPPING AND CONCLUSIONS

Fumio Furuta, Ralf Eichhorn, Mingqi Ge, Daniel Gonnella, Don Hartill, Georg Hoffstaetter, John Kaufman, Matthias Liepe, Eric Smith, Cornell University, Ithaca, NY 14850, USA

Abstract

Multi-cell temperature mapping (T-map) system for 1.3GHz SRF Nb cavities has been developed at Cornell. T-map system consists of nearly two thousand thermometers array positioned precisely on an exterior cavity wall and is capable of detecting small increases in temperature. It has achieved a 1mK resolution of niobium surface temperature rinsing in superfluid liquid helium. We have upgraded the system to be capable of monitoring the temperature profiles of quench spot on cavity. The recent results of T-map during cavity tests and details will be reported.

INTRODUCTION

T-mapping history can be traced back to the 1980s. Cornell University was a pioneer in developing a 1-cell T-map system for 1.5GHz SRF cavity research [1, 2, and 3]. Now Jefferson Lab and Fermilab also have 1-cell or 2-cell T-map systems. These systems are used for fundamental SRF research via single-cell cavities. Due to the requirement on further understanding of multi-cell cavities, the development of a multi-cell T-mapping system becomes more necessary and ultra-important. DESY and Los Alamos have multi-cell T-mapping systems for ILC 9-cell cavities [4, 5]. Those systems are mainly used to detect quench location.

The Cornell multi-cell T-mapping system, by virtue of its high sensitivity, is able to detect heating levels much lower than those required to cause a quench. The hot-spots normally start in the medium accelerating gradient region and cause a Q-drop. Increasing the accelerating gradient of cavity, the heating at a hot-spot will grow as well, and eventually quench the cavity. Therefore it is important to discover not only the quench location but also the original location of heating as well as the growth of the heating rate versus accelerating gradient. This information would help to unveil the loss mechanism of superconductivity under medium RF field, and address fundamental physics..

MULTI-CELL TEMPERATURE MAPPING SYSTEM

Cornell multi-cell T-map system has been developed for the 7-cell cavities of Cornell ERL project. This system could also fit onto 1.3GHz TESLA shape 9-cell cavities, and covers the centre 7-cells of 9-cell. We did several trials of T-map with 9-cell cavity to confirm the performance of system. The details of them will be described later. The additional boards are under fabrication for the full 9-cell T-map system. The cavity specification values of Cornell ERL 7-cells are quality factor (Qo) of 2×10^{10} at accelerating field gradient of 16MV/m in 1.8K [6]. The temperature rise of ~20mK on the exterior wall is estimated against a 1.3GHz SRF cavity with Qo of 2.0e10 at 16MV/m in 2.0K helium bath [7]. The sensor is able to detect the temperature rise of the cavity wall with 25% efficiency [3]. Thus the resolution of this T-map is required to be approximately 1mK.

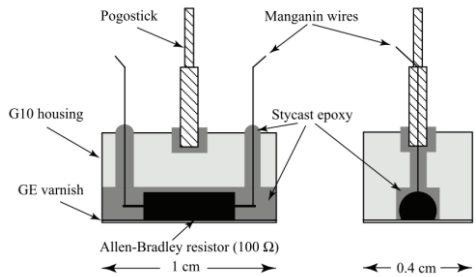

Figure 1: Thermometer schematic [3].

Thermometers and Boards

The temperature sensors are a 100Ω carbon Allen-Bradley resistor (5% 1/8 W). Carbon is a semiconductor, its resistance increases exponentially when temperature drops. Figure 1 shows the schematic of sensor and its picture. The system consists of two sets of 3-cell boards and one set of 1-cell boards, so it covers 7-cells in total. The sensor boards are spaced azimuthally every 15° around the cavity; totally it has 24 boards per cell around the azimuth. Each board has 11 thermometers per cell, so each cell is covered by an 11×24 thermometer array. The quantity of thermometers for the whole 7-cell cavity is 1848. Dow Corning vacuum grease was applied on the varnished side of the thermometers prior to inserting the boards in cages. Silicone-based Dow Corning grease has similar thermal conductivity to traditional APIEZON grease in superfluid helium, but much cheaper than APIEZON grease. When the thermometers press to the cavity wall, the grease spreads into remaining gaps and

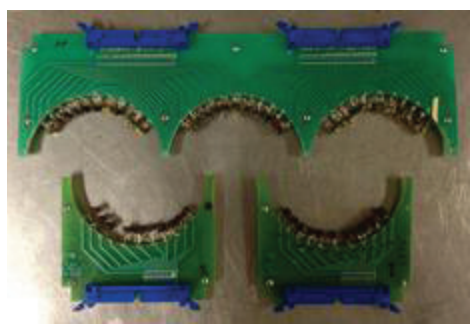

Figure 2: A 3-cell board and 1-cell boards.

*This work has been supported by NSF award PHY-0969959 and DOE award DOE/SC00008431

ISBN 978-3-95450-178-6

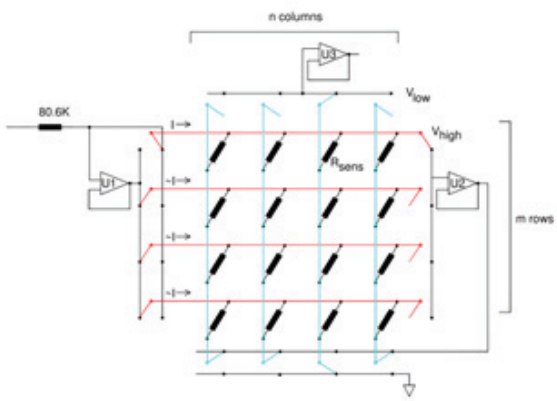

Figure 3: New scheme for multi-cell T-map.

prevents superfluid helium from cooling the sensors. Figure 2 shows a 3-cell and a 1-cell board. A 3-cell board has two channels addressed to the sensors for 3-cells.

Electronic and Scan Scheme

The traditional scan-scheme for single-cell T-map has two wires on each sensor. A multiplexer scans each sensor one by one. Therefore the number of wires is double the number of sensors. However, for a multi-cell T-map application the wire numbers would reach approximately four thousand if that single-cell T-mapping scheme were adopted. A simple scheme was proposed [8] to reduce wire numbers. Figure 3 illustrates the schematic of a new scan scheme for a multi-cell T-map.

In the conceptual view of Figure 3, the working principle of the multi-cell scheme is shown. Each of an array of m×n resistive thermal sensors has one lead attached to a "column" wire, and one lead attached to a "row" wire. In the case of our implementation, there are 24 columns and 11 rows in each array. Each column wire may be connected by a CMOS switch to an operational amplifier (U3), and by a low-on-resistance CMOS DPDT switch to either ground or to the output of op-amp U2. Likewise, each row wire may be connected by a CMOS switch to the input of the follower op-amp U2, and through a low-on-resistance CMOS DPDT switch to either a current source or to the output of op-amp U2 which tracks the output voltage of the current source. In a measurement of a particular sensor, the column wire for that sensor is connected to U3 and the system ground, while the other column wires are connected to the output of U2, while the row wire for that sensor is connected to the current source and the input of U2 and the output of U1. Thus all the rows and all but one of the columns are at the same potential (neglecting the wiring resistance), and a current given by the current flows through the selected resistor. There is a current of similar magnitude, though depending in detail on the resistance of the other sensors, through all of the other sensors on this same column. The resistance of the selected sensor is determined by the voltage difference between the output of U2 and U3. It is necessary to keep the measurement voltage relatively small to avoid overheating of the sensor

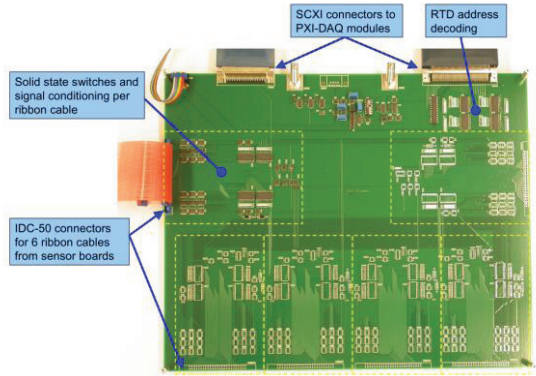

Figure 4: Picture of signal processing board [8].

by the measurement power. We use a current source providing about 4 microamperes through the nominal 10K sensor resistance at the operating temperature, giving approximately 40mV of "typical" signal across a sensor. To get meaningful readings, the op-amps used in the circuit must be very low in voltage offset (ca. 1 microvolt), or else the unintended currents through the other resistors in the array will cause unacceptable errors. In our case, we use 5×IDC-50-wire cryogenic ribbon cables (250 wires in total) for 1848 thermometers.

The analog sensing and digital control for the signal processing board is provided by a National Instruments PXI-1033 chassis. In the chassis is a PXI-6123, 8-channel analog input, 500 kHz DAQ module, and a PXI-6509, 96 DIO module for thermometers addressing, signal conditioner gain select, carrier waveform select, and reference thermometer control. A Matlab code on a Windows PC with a PCI slot controls the PXI chassis.

The switching and signal processing board fabricated for multi-cell cavity is shown in Figure 4. It is an 8-layer board with surface-mount components on both sides. There is a section for decoding the thermometer address and 6 duplicated channels to process the signals from 6 ribbon cables.

Insert for Cryogenic Test Pits

Cornell constructed a new test insert for hanging the multi-cell cavity with full T-map. Figure 5 shows the Cornell multi-cell T-map attached on middle 7-cells of a 1.3GHz 9-cell cavity (left) and some cross section (right). The insert has a feedthrough on the top-plate for extracting T-mapping cables out of the Dewar. A coupler motor and Ion pump were built on the insert as well, which allows us to adjust the coupler position as well as to keep the cavity under high-vacuum during the RF test. Three well-calibrated Cernox thermometers were attached on the insert for T-map calibration.

SYSTEM EVALUATION

We did commissioning test of multi-cell T-map system with a 1.3GHz TESLA shape 9-cell cavity. The cavity was prepared with 5um vertically electro-polishing

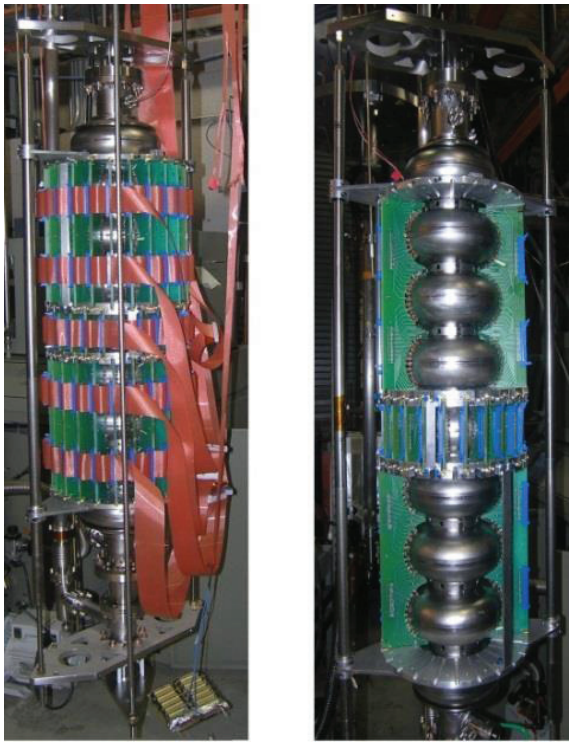

Figure 5: Picture of cryogenic insert with T-map.

followed by high pressure water rinsing. No 120°C baking was applied on the cavity for the test.

Calibration and Sensitivity

A well-calibrated Lakeshore Cernox thermometer is utilized as a temperature reference for the helium bath during cooling down from 4.2K to 1.6K. Figure 6 is a sensor's calibration curve. The X-axis is the resistance value of the carbon resistor, and the Y-axis is the reciprocal of the temperature measured by the Cernox sensor.

A polynomial function was adopted to fit the curve, shown in equation (1).

$$\frac{1}{T} = a_n x^3 + b_n x^2 + c_n x + d_n \qquad (1)$$
$$x = ln(R)$$

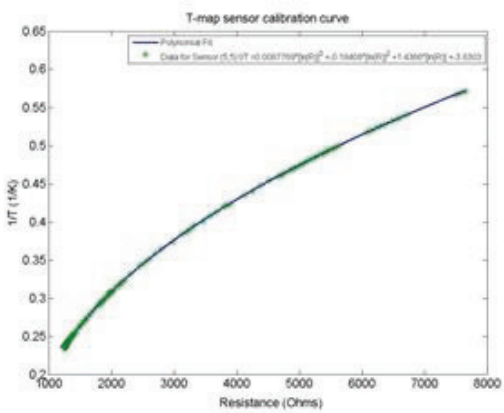

Figure 6: 1/T vs. Resistance curve during cooling down.

Here T is the bath temperature, R is the resistance of the carbon resistor, a_n, b_n, c_n, and d_n are fitting parameters for sensor n. To avoid measurement error caused by bath temperature variation, the data-scan program measures bath temperature right after each T-mapping sensor measurement. Therefore each Allen-Bradley resistor has an individual calibration curve and fitting parameters. Each resistor's thermal performance is slightly different from one to another.

By using fitting curves, it is possible to calculate $\frac{dR}{dT}$ which represents the sensitivity of each T-mapping sensor. An Allen-Bradley resistor value is about 12kΩ at 1.6K, $\frac{dR}{dT}$ is approximately 30Ω/mK; and $\frac{dR}{dT}$ is about 10Ω/mK at 2K.

Noise Level Analysis

Noise comes from the environment and the electronic system. Good grounding of all instruments helps to reduce noise from environment. We use a grounding line to connect the signal generator, RF amplifier, T-mapping electronics, and Dewar together with a building grounding point.

Increasing measurement sampling number is an effective way to reduce noise from the electronic system. The PIXI controller can sample the sensor voltages at a 500 KHz rate, and average readings for 2^N samples. The N is the parameter for setting sampling number in the Matlab program. The program returns average value of each thermometer. Figure 7 shows the standard deviation of resistance decreasing with increasing sampling number. Each point in Figure 7 was calculated from 10 scans at different N value. The dash line in the plot is a theoretical curve which is the standard deviation versus $\sqrt{1/2^N}$.

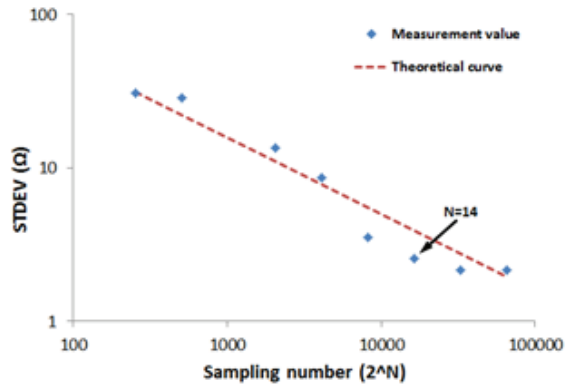

Figure 7: Standard deviation vs. sampling number.

The standard deviation is reduced to about 2Ω, when N is set to 14, corresponding to a sampling number of about 16000. We don't choose a higher N value because higher N will significantly extend scan time. The noise from the electronic system is about 200μK in a 2K helium bath; and 67μK in 1.6K helium. The total scan time is about 100s.

Thermal conductivity of grease as well as press-force of sensor against cavity-wall affects T-map noise level as well. Figure 8 is a lateral view of the subtraction between

ISBN 978-3-95450-178-6

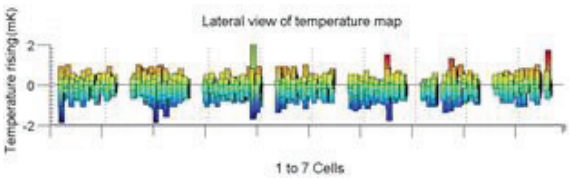

Figure 8: 3-sigma noise level of T-map system. The one sigma noise is only about 0.2mK.

two T-map scans without applying RF field in 2K Helium bath. The total noise of the T-map system is about 1mK which achieved our initial goal. Work continues on improving temperature stability of the helium bath, which may be the present limit on system temperature noise.

CRYOGENIC TEST

Hot Spot Detection near Quench Field

The 9-cell cavity A9 was tested in a 2K helium bath and quenched at 21MV/m in pi-mode. The T-mapping boards covered the middle 7 cells of the cavity. Temperature-map data was taken at an accelerating gradient very close to quench. Figure 9 depicts the temperature-rise (ΔT) map. The T-mapping result is a 3D bar plot in which the x-axis and y-axis are the coordinates of T-mapping sensors and the z-axis is ΔT. In Figure 9, the left plot is the top view of the T-map result, each blue rectangular area represents a thermometer array attached on a cell, and has same sequence with cavity cells from top to bottom; the ΔT is showed by colours. The right plot is an isometric view of the T-map with a finer scale (0-15mK) of ΔT which better displays tiny heating on cells.

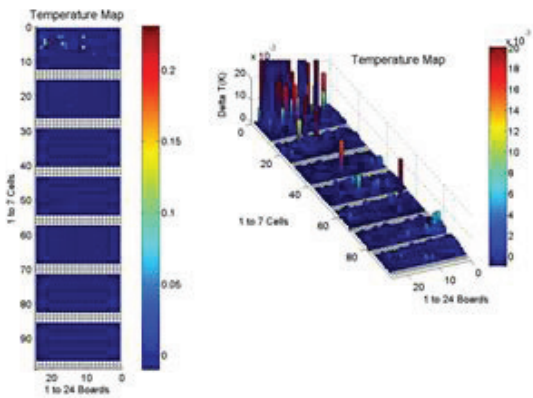

Figure 9: Map of temperature increase for 7-cells of an ILC cavity. The dominantly heated cell at fields close to quench is clearly visible.

Cooling Front Monitoring

By modifying the T-map data sampling program, the system could monitor the detail profile of temperature distribution on cavity outer surface during the cool down. Figure 10 shows an example of T-map results during the fast cool. The fast cool means cavity was cooled down very quickly with huge temperature gradient between top and bottom cell in vertical test dewar, >100K. In Figure 10, the bottom half of cavity had already reached

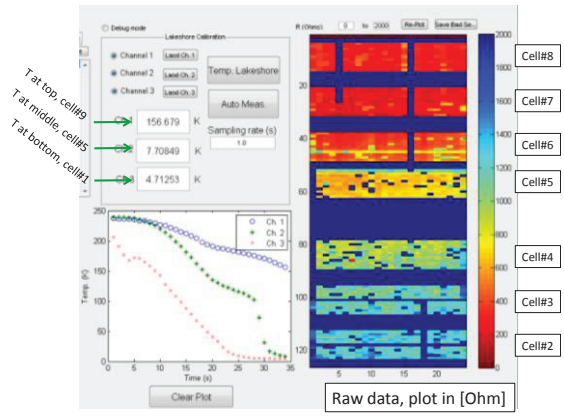

Figure 10: Cooling front monitoring with 9-cell.

4.7~7.7K, below Tc, but top of the cavity was about 157K, still stayed in normal conducting. This monitoring will allow us to see the actual temperature uniformity on cavity surface and temperature gradient at the boundary of normal and super on cavity.

Quench Localization

Hot spot detection could predict the quench location on cavity. By inputting the address of hot spot sensor location to the T-map program, the program could keep monitoring the temperature change of hot spot during the quench. Several temperature profile monitoring was performed against several hot spots. The hot spot which showed the highest temperature change during the quench was identified as quench spot. Figure 11 shows an example of quench detection with T-map. Figure 12 shows the detail profile of the signal. Quench location

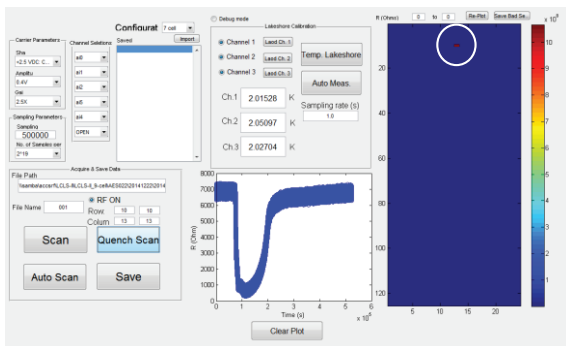

Figure 11: Quench localization.

was also predicted by 2nd sound detections with OSTs.

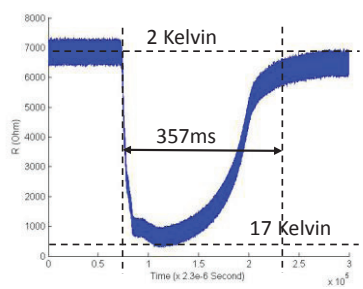

Figure 12: Quench signal detail.

Two different detections, T-map and OST, predicted the same quench spot. Optical inspection was done after cavity test, it turned out that there was the defect on quench spot predicted by T-map and OSTs. Figure 13 shows the summary of quench detections and optical inspection image of defect. The combination of these three system, T-map, OST, and optical inspection, is very strong tool as the quench localization and could provide more information to investigate quench mechanisms.

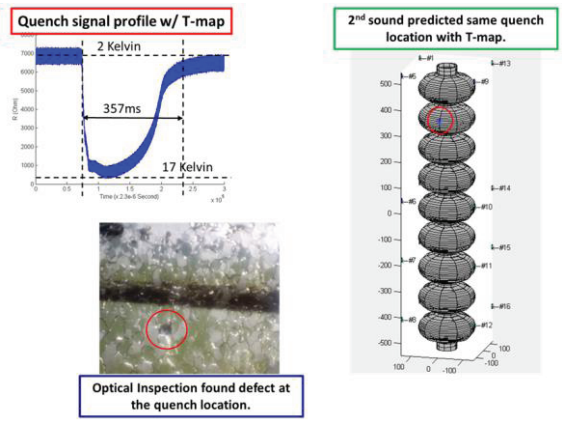

Figure 13: Quench localization with T-map, OST, and optical inspection.

CONCLUSIONS

Cornell multi-cell T-map system has been developed and successfully tested on multi-cell cavities in 2K helium bath. The system had achieved 1mK resolution in 2K helium bath. Multi-cell T-map system becomes more functional by upgrading the control programs. The system is capable of not only detecting hot spot, but also monitoring cooling front during the fast cool, detecting quench signal with time profiles. The combination of T-map, OST, and optical inspection is very strong tool to investigate cavity quench phenomena. Further R&Ds with these tools are expected to bring more understandings of Nb SRF cavities. More effort on converting T-map data into Qo-map of Nb cavity surface is ongoing.

REFERENCES

[1] H. Padamsee et al., "Field Emission Studies in Superconducting Cavities", PAC'89, Washington D.C., p. 1824.

[2] P. Kneisel, G. Mueller and C. Reece, "Investigation of the Surface Resistivity of Superconducting Niobium Using Thermometry in Superfluid Helium", 1986 Applied Superconductivity Conf., Baltimore, MD.

[3] J. Knobloch, Ph. D. thesis, CLNS THESIS 97-3(1997). http://www.lns.cornell.edu/public/CESR/SRF/dissertations/knobloch/knobloch.html

[4] Q.S. Shu, et al., "An Advanced Rotating T-R Mapping & It's Diagnoses of TESLA 9-Cell Superconducting Cavity", PAC'95, Dallas, TX, p.1639.

[5] A. Canabal, et al., "Development of a Temperature Mapping system for 1.3-GHz 9-Cell SRF Cavities", PAC'07, Albuquerque, NM, p. 2406.

[6] M. Liepe et al., "Progress on Superconducting RF Work for the Cornell ERL", WEPPC073, IPAC 2012.

[7] http://arxiv.org/abs/1405.4226

[8] E. Chojnacki, "A multiplexed RTD temperature map system for multi-cell SRF cavities," SRF2009, 2009, TUPPO033, p. 276.

ISBN 978-3-95450-178-6